Tunnelling and Underground Space Technology 141 (2023) 105391

Contents lists available at ScienceDirect

Tunnelling and Underground Space Technology incorporating Trenchless Technology Research

journal homepage: www.elsevier.com/locate/tust

Back-analysis of sprayed concrete lined (SCL) tunnel junctions at Liverpool Street Crossrail station

Alun Thomas [a,*], Nicholas de Battista [b], M. Elshafie [c], G. Viggiani [d]

[a] All2plan Consulting ApS, Denmark
[b] Epsimon, United Kingdom
[c] Qatar University, Qatar
[d] University of Cambridge, United Kingdom

ARTICLE INFO

Keywords:
Sprayed concrete lined tunnels
Junctions
Fibre optic monitoring
Numerical modelling

ABSTRACT

Sprayed concrete linings (SCL) offer a versatile method of tunnel construction, particularly in regard to forming junctions since the lining acts as a shell structure which can redistribute the stresses around the opening efficiently. This process is easy to understand conceptually but it is much more difficult to illustrate in calculations. Conventional calculation methods make a number of far-reaching simplifications such as the assumption of linear elastic behaviour in the lining. This often leads to overly conservative designs and a residual concern over the loads in the lining. This study compares detailed measurements of strains recorded by distributed fibre optic sensors at a pair of junctions on the Crossrail project in London with a sophisticated numerical model of these tunnels. Having demonstrated that the results of the numerical model are broadly consistent with this unique set of field data, a variety of influences on the model have been examined. This includes the excavation sequence, the constitutive model for the lining and adjacent structures. The results indicate significant scope for the improvement of SCL junction design. Future papers will present the more results from other parts of this study along with their implications for the design of tunnel junctions.

1. Introduction

Sprayed concrete linings (SCL) offer a versatile method of tunnel construction, for both hard rock and soft ground (ICE, 1996; Thomas, 2019). SCL tunnels can be constructed in a wide variety of sequences and shapes as well as being combined with additional support measures. Consequently, this method of tunnelling has become increasingly popular, particularly for geometrically complex structures such as the many tunnel junctions in metro stations.

The behaviour of the lining is more complicated than for other types of tunnel lining. This is partly because the properties of the concrete change substantially in the early period when the lining is also being loaded by the ground. In contrast a segmental lining is loaded when the concrete is mature which is the usual case for reinforced concrete structures. Hence with the versatility that SCL offers comes an increased complexity in design. This is especially true in the case of tunnel junctions. The lack of detailed field data from junctions has added to the sense of uncertainty about the actual behaviour of the lining. Without wishing to overstate this uncertainty, this can lead to both over-design and under-design, as evidenced by a wide variation in the level of support and reinforcement applied at junctions in similar ground conditions and, on the other hand, some rare examples of tunnel collapses at junctions where design errors have been a contributory factor.

As a step to address this lack of field measurements, distributed fibre optic sensors were installed around two junctions in a project in London. This paper will describe the limitations in our understanding of SCL junction behaviour and the current design tools. The monitoring program will be described. A high quality set of data was obtained for strains around the junctions during their construction. A program of numerical modelling with a sophisticated 3D model has been undertaken to back-analyse these field measurements and explore areas of improvement for SCL junction design. The program included various constitutive models for the lining, construction sequences, modelling techniques and both short and long term behaviour. As the first in a series of planned papers, some of the findings from this work from the short term analyses will be presented here.

* Corresponding author.
E-mail address: info@all2plan.com (A. Thomas).

https://doi.org/10.1016/j.tust.2023.105391
Received 17 November 2022; Received in revised form 8 July 2023; Accepted 3 September 2023
Available online 7 September 2023

1.1. Field measurements

Crossrail (now named The Elizabeth Line) is a railway line in London, running from West to East, and passing under the city's centre (Thomas, 2021). This was the first major addition to the London metro system since the Jubilee Line Extension (opened in 1999) and the first completely new line since the Docklands Light Railway (opened in 1990). During Crossrail's main construction period from 2011 to 2017, the £18 billion project was the largest construction project in Europe.

Of the 39 stations linked by the Crossrail route, five of these were excavated under central London, using the Sprayed Concrete Lining (SCL) method. The underground stations typically consist of short concourse tunnels in between two platform tunnels, all linked with a number of cross-passages. The permanent lining of these station tunnels is formed of sprayed concrete.

The challenges of designing SCL tunnels in soft ground are well documented (HSE, 1996; ICE, 1996; Jones, 2007; Thomas, 2019) and the design of junctions is particularly difficult. For this reason, in addition to the normal monitoring of lining convergence and ground movements, a distributed fibre optic sensor (DFOS) system was embedded within the concourse tunnel lining at one set of junctions at Liverpool Street Station – between a concourse tunnel (CH5) and two cross-passages (CP1 and CP2) – see Fig. 1. The arrangement of these sensors was designed to record the changes in strain that occurs within the lining during the breaking out and excavation of the cross-passages – see section 2. Despite the challenges of installation, high quality measurements of the strains in the lining during cross-passage construction were obtained (de Battista et al., 2019).

1.2. Tunnel junction design

While junctions (between tunnels or between a tunnel and a shaft) are a common feature of underground infrastructure. They are known to be difficult to analyse in design and there has been relatively little research into their behaviour. This is particularly true for SCL tunnels, despite the fact that the sprayed concrete redistributes the stresses in the larger ("parent") tunnel more efficiently around the opening for the "child" tunnel than a segmental lining. SCL acts as a shell structure, permitting the stresses to arch around the opening (see Fig. 2). This leads to concentrations of compression on either side of the opening, due to the channelling of the dominant force – the hoop force (Jones, 2007; Chortis & Kavvadas, 2020). Similarly, the longitudinal forces arch around the tunnel. However, these are usually much lower than the hoop forces, so the impact is less significant. Above and below the openings, tension can develop, either in the longitudinal direction due to the divergence of the lines of hoop force or in the hoop direction for a number of reasons which will be discussed later.

These basic concepts have been well understood for many decades. Simple design methods such as the "hole-in-an-elastic-plate" analytical solution have been used (Thomas, 2019). These have been shown to have significant limitations, which is unsurprising given the highly three dimensional nature of the situation. Also these methods cannot simulate the actual excavation sequence and the lining is assumed to be linear elastic. In practice, tunnellers have been able to construct SCL junctions safely with large aspect ratios, approaching 1.0, in soft ground as well as in rock, despite the calculations which often predicted severe overloading of the lining (e.g. Grose & Eddie, 1996 vs Hafez, 1995). This

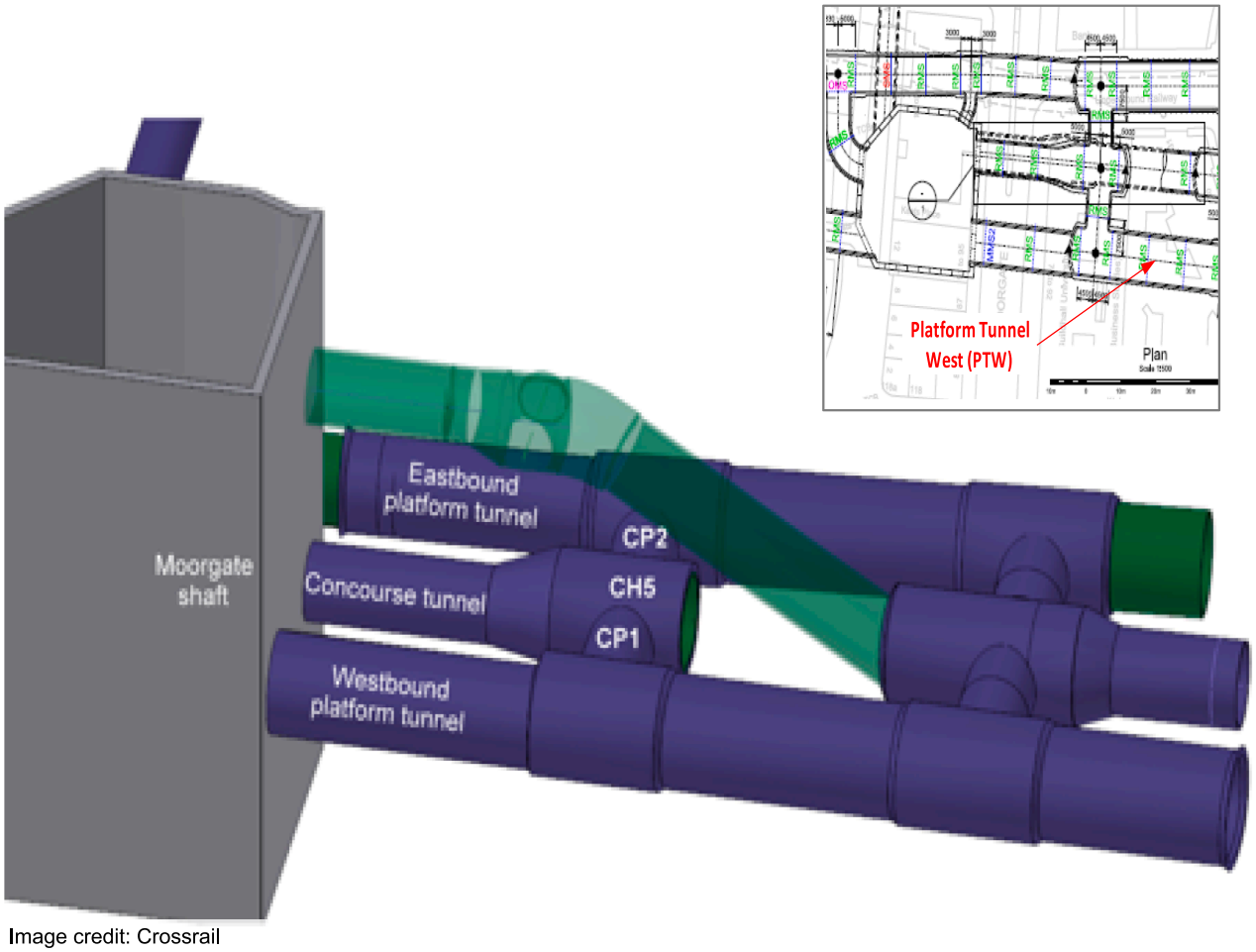

Fig. 1. General arrangement of the tunnels at Liverpool Street Station, showing the instrumented junctions at the concourse tunnel (CP1-CH5-CP2).

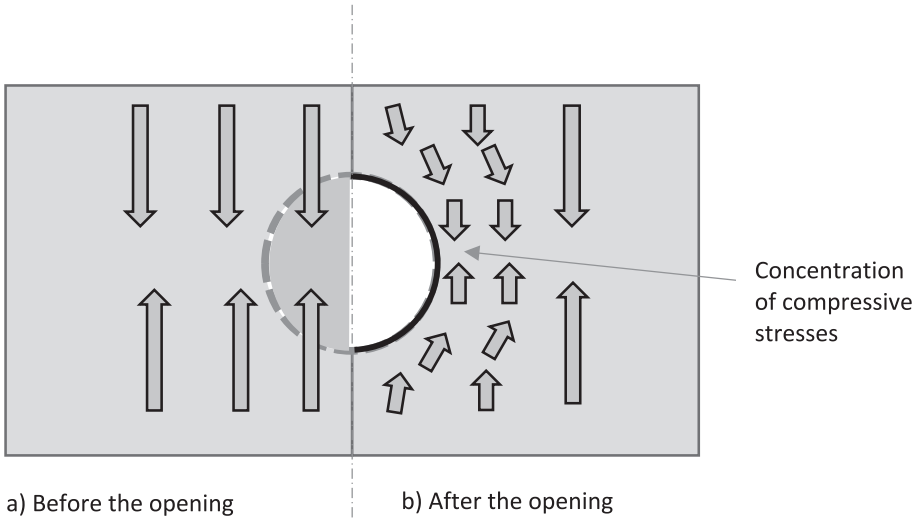

Fig. 2. A schematic of the hoop forces arching around an opening in an SCL tunnel.

implies that current calculation methods lead to some degree to overly conservative designs.

Early studies using numerical models (e.g. Kropik, 1994; Hafez, 1995) were hampered by the limits on computing power at the time. Nonetheless they were able to show the arching of the stresses around an opening, as envisaged in the conceptual model. As computing power has increased, so has the use of 3D numerical models to design junctions (e.g. Goit et al., 2011; Diez, 2018). While there are some published articles on this subject (e.g. Goit et al., 2011; Diez, 2018; Chortis & Kavvadas, 2020), few of them compare the results of the models with analytical solutions or monitoring data from real tunnels. Hence considerable uncertainty remains over the actual state of stress at a junction and this explains the high degree of conservatism in current designs.

One notable exception is the work carried out by Jones (2007) who modelled in detail the construction of an SCL tunnel from an SCL shaft in London clay at Heathrow airport. The 3D numerical model results were compared with a range of monitoring data from the ground and the lining, as well as the analytical solution for a hole in a plate. One conclusion was that the modelling of the parent structure – in that case a shaft – could be simplified down to a two step process using the relaxation method, whereas it was important to simulate each construction step of the child tunnel. Typically each construction step in this type of soft ground is 1 m in length so for a 20 m deep shaft, the calculation steps can be reduced from 20 to 2, with a considerable saving in computing time. Jones (2007) obtained a reasonable agreement with both surface settlement and lining stress measurements, albeit based on limited data, by using a sophisticated nonlinear elastoplastic model and a detailed simulation of the construction sequence.

Other studies have employed simplifications in the models – either for the ground, the sequence, or the lining – and consequently the agreement with measured data has suffered. As an example, Li et al. (2016), who modelled very large tunnels (the face area of the parent tunnel was 400 m^2) in a weak rock stratum, appear to have over-predicted lining movements by a factor of two but the predicted lining hoop stresses seemed to agree better with measurements. However, whereas these stresses would indicate overloading of the tunnel and the corresponding predicted hoop axial forces and moments indicated that the capacity of the lining was exceeded, there is no mention of damage during construction. Gakis et al. (2016) rightly emphasized the importance of back-analysis as a means of learning from success and feeding this back into the designs. Their back-analysis considered junctions at the Crossrail Farringdon station. Since they used a simple linear elastic-perfectly plastic constitutive model for the ground, an unrealistically low K0 value of 0.6 was needed to obtain a reasonable agreement with surface settlement data. There is no discussion in the paper about the comparison with other geotechnical monitoring or the lining behaviour.

Chortis & Kavvadas (2020) present the results from an extensive parametric study of a hypothetical cruciform shaped junction in rock. In addition to varying parameters such as depth, rock mass stiffness and strength, aspect ratio of the junction and K0, a variety of construction sequences were also investigated. In common with most studies, a simple linear elastic model was used for the lining. Amongst the conclusions, it was observed that the first few metres of the break-out from the parent tunnel had the most impact and that breaking out had a more severe impact than an approaching a tunnel. The changes in lining stresses reduced considerably as the strength of the ground increased. The authors proposed a set of design charts. However, these only predict the changes in axial forces, whereas in fact bending moments often tend to govern the design of the reinforcement needed at junctions.

The original design of the junction in this case study, at Crossrail Liverpool St station, was based on a set of design charts covering axial forces and bending moments in both the hoop and longitudinal directions (Diez, 2018). These charts were developed from a parametric study using a sophisticated 3D numerical model (Thomas, 2021). The design charts provided "concentration factors" which were used to multiple up the loads predicted by 2D models of the parent tunnels to account for the concentration of loads at junctions (see section 3). While the numerical models had a sophisticated constitutive model for the ground, including depth varying parameters and nonlinear elasto-plastic behaviour, the modelling of the lining was more simplistic. Linear elasticity was assumed for the lining elements and main analyses assumed a constant stiffness, although the effects of ageing for the cross-passage were also checked. A simplified, two step process was used for the construction of the parent tunnel while each advance length for the cross passage was simulated. The overall modelling procedure for the original design had been calibrated against a range of field measurements (in general for tunnels without junctions) from two case studies of similar SCL tunnels in London (Goit et al., 2011).

Despite the uncertainties surrounding SCL behaviour junctions, hardly any field monitoring data are available from these structures to feed back into the design methods. It is common practice to record displacement and convergence measurements of the tunnel lining intrados using optical surveying instruments. However, these do not give a direct measurement of the changes in stresses and strains occurring within the lining, and are therefore more useful for the day to day monitoring of safety in tunnel construction rather than for model validation. Pressure cells have been embedded occasionally within SCL to measure the stress within the lining or at the soil-lining boundary (van

der Berg, 1999; Jones, 2007). However, these are difficult to install within SCL and they only provide point measurements of strains at discrete locations. In addition, the data obtained from embedded pressure cells are difficult to interpret accurately as the measurements are affected by installation effects, temperature changes and concrete shrinkage (Clayton et al., 2000, 2002; Jones and Clayton, 2020).

In summary, while there is general agreement on how SCL tunnels are believed to perform at junctions, there is very little monitoring data to confirm this. In addition, some of the assumptions adopted in the designs deserve to be challenged and validated. Without conducting such an exercise, a question mark will remain hanging over the uncertainty in the results of the numerical modelling of SCL junctions, no matter how sophisticated these models might appear to be. The objective of the DFOS instrumentation and monitoring campaign carried out at Crossrail Liverpool Street station was to provide reliable monitoring data to enable the tunnel lining behaviour to be back-analysed, thus providing valuable information for future designs.

2. Fibre optic instrumentation and monitoring of the SCL

2.1. Arrangement and installation of fibre optic strain sensors

The enlargement chamber CH5, located at the west end of the Crossrail Liverpool Street Station, was instrumented with a distributed fibre optic sensor (DFOS) monitoring system. DFOS is a relatively new instrumentation technology that enables strain to be measured at closely spaced intervals from FO cables embedded or attached to a structure (Kechavarzi et al., 2016). As stated earlier, the objective was to measure directly the spatially distributed pattern of strain changes in hoop and longitudinal strain profiles that occur within the SCL of the parent tunnel during the various stages of breaking out and excavation of a cross-passage (CP). DFOS provides a much richer data set than conventional point sensors, which is crucial for back-analysing the SCL design and validating the model assumptions.

The installation was carried out during May 2014, before the concourse tunnel was connected to the platform tunnels on either side, with cross-passages CP1 and CP2 (see Fig. 1). The layout of DFOS cables is shown in Fig. 3. This consisted of four sections:

- Two rings (T1 and T2) around the circumference of the tunnel, one on either side of the CPs, approximately 0.5 m away from the CPs at the closest point
- Two rectangles (e.g. L1-L2-L3-L4) on the sides of the tunnel, one around each CP, with the longitudinal parts being approximately 0.5 m above and below the crown/invert of the CPs. The circumferential parts were approximately 2.0 m to the side of the CPs (i.e. 1.5 m away from the DFOS rings).

For safety reasons, it was not permitted to install the cables until a sufficiently thick and strong lining had been installed to create a safe working environment. Furthermore, because of the stepped, sequential nature of the excavation of CH5, which consisted of a top heading, bench

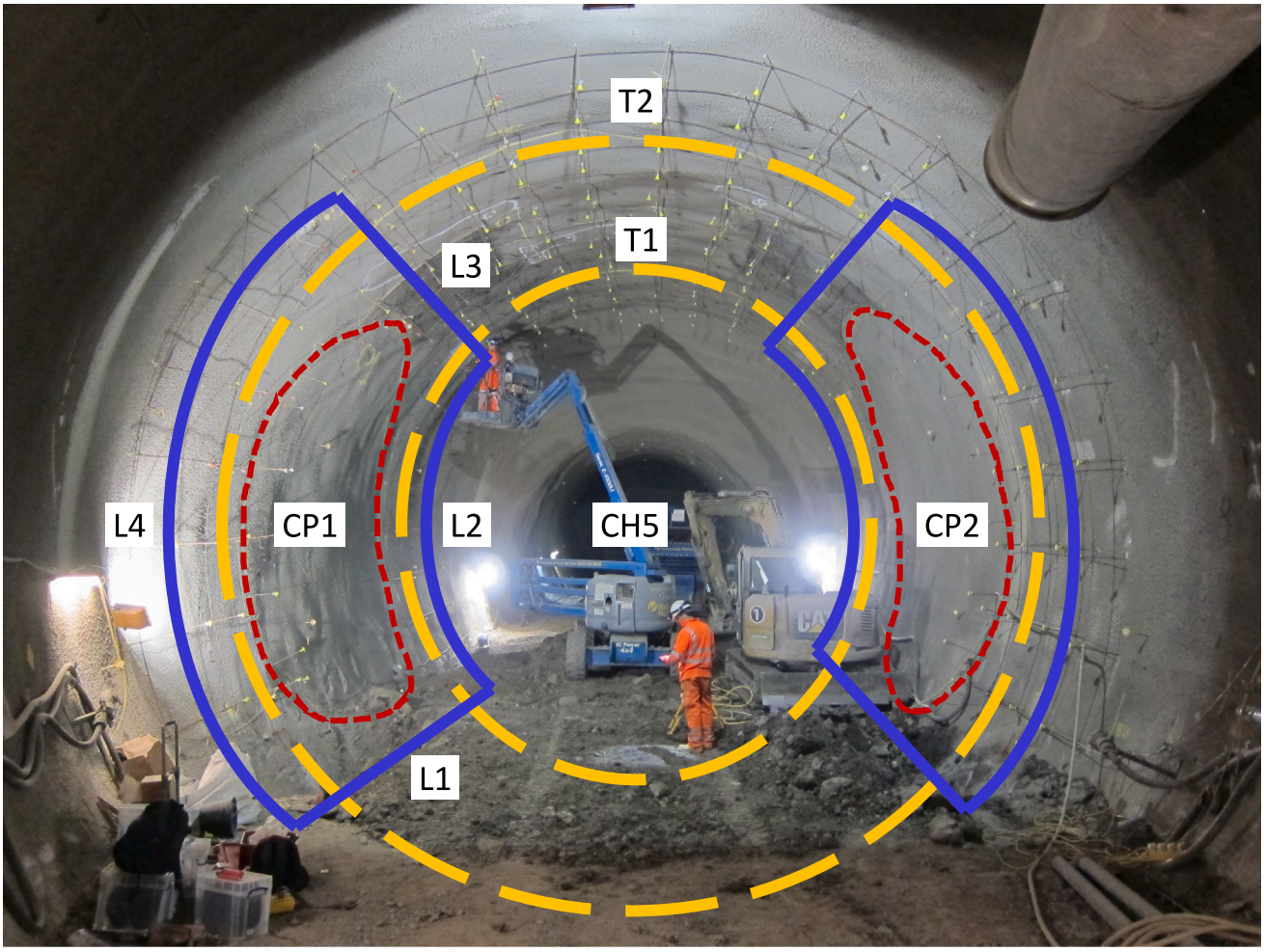

Fig. 3. The planned layout of the embedded DFOS instrumentation, consisting of two rings (shown in orange dashed lines) on either side of the cross-passages and two rectangles (shown in blue solid lines) around CP1 and CP2. (For interpretation of the references to colour in this figure legend, the reader is referred to the web version of this article.)

and invert sequence, it would have been physically very difficult to install these closed loops of cables while that tunnel was being excavated. The stress state in a individual SCL tunnel is relatively well understood (e.g. van der Berg, 1999; Thomas, 2003; Jones, 2007 & Thomas, 2019). The focus here was on the change in stress and strain in a tunnel due to the construction of the junctions. Therefore, it was decided to install the cables while the additional reinforcement and thickening of CH5 was being installed, prior to the excavation of the cross passages.

Soon after installation, the cables in the rectangle around CP2 were damaged and could not be repaired. Therefore, the final monitoring system consisted of the two circumferential rings and the one rectangle around CP1.

Each of the DFOS sections described above comprised two fibre optic (FO) sensing cables installed side by side: one cable to measure temperature (single mode Excel 8-core 9/125 OS1) and another cable to measure the combined effects of strain and temperature (single mode Fujikura 4-core 9.5/125 JBT-03813). The FO cables were attached directly (externally) onto the 400 mm thick primary SCL layer. Subsequently, an additional 400 mm thick primary thickening SCL layer was sprayed, such that the FO cables were embedded within, and approximately in the middle of, the combined 800 mm thick SCL layer. The ends of the individual cables were then joined together with fusion splices contained within a FO connection enclosure a few metres away from the installation, resulting in one complete circuit of DFOS cables. This circuit was connected to an armoured FO routing cable to enable measurements to be taken from a monitoring cabin placed in a safe location within the tunnel, around 50 m away from CH5. Further details about the instrumentation, monitoring and the working principles of DFOS are provided by [2].

A consequence of the installation is that the cables lay approximately in the middle of the section of the lining, so that, at best, they could only record the average strain changes in the lining. That assumes that the two parts of the primary lining act together as a perfect composite structure – as intended in the design. While both consist of the same sprayed concrete, the layers were sprayed at different times and so they had slightly different stiffnesses when the cross passages were built. The thickening (and instrumentation) was installed in May 2014, several months after CH5 was completed, and cross passage construction began in June 2014. The movements (and therefore stress state) in the primary lining were stable before the thickening was applied. Typically the rate of increase in stiffness for sprayed concrete is very slow after 28 days (Thomas, 2019) so it is a reasonable approximation to assume that both parts of the lining had a similar stiffness, close to the 28 day value. This stiffness is much higher than both the fresh sprayed concrete of the cross passage when it is first built and even higher than the surrounding ground. As noted in the conclusions of this paper, bending moments are important in determining the design of a lining at a junction. Installing a similar arrangement of DFOS cables at various depths throughout the lining would yield extremely valuable information on the behaviour. However, for the safety reasons explained earlier, on this occasion, this was not possible.

2.2. *Monitoring of fibre optic strain sensors*

Monitoring of strain and temperature from the embedded DFOS cables was carried out using a Yokogawa AQ8603 Brillouin optical time domain reflectometry (BOTDR) analyser located in the monitoring cabin. The tunnel lining was monitored during three periods between June and August 2014, which coincided with the breaking out and excavation activities of the pilot and enlargement tunnels of the two CPs in CH5. Each monitoring period started a few days before, and continued until a few days after, the excavation activities of the particular period. A fourth monitoring period was also carried out when no excavation activities were happening within CH5, between the completion of CP1 enlargement tunnel and the start of CP2 enlargement tunnel.

Measurements were taken once every 15 min during the first two monitoring periods (CP pilot tunnels and enlargement of CP1) and every 30 min during the last two monitoring periods. Temperature-compensated strain readings were obtained at 0.1 m intervals along the instrumentation lines. Due to logistical difficulties, the very first measurement (the baseline measurement) could not be taken until after the CP1 pilot tunnel was broken out. Consequently, all the measurements recorded from the DFOS system provide the change in strain that occurred in the tunnel lining after CP1 pilot tunnel break-out.

Fig. 4 provides a graphical representation of the strain change profile recorded within the tunnel lining after the completion of both CPs. In the hoop direction a maximum increase in compressive strain of 820 με was recorded close to the side of CP2, whereas in the longitudinal direction a maximum increase in tensile strain of 567 με was recorded directly below the invert of CP1. The monitoring results are reported in more detail by de Battista et al (2015).

3. The original design

The sprayed concrete linings for Crossrail were designed by Mott MacDonald. An overview of this innovative design can be found in Thomas (2021). The key innovative features can be summarised as the follows:

- Permanent sprayed concrete for all tunnels (including public areas)
- Fibre reinforcement only – except in exceptional cases such as junctions
- Spray applied waterproofing membrane

SCL is ideal for forming junctions since it functions as a shell structure and therefore it can efficiently re-distribute the stresses in the parent tunnel lining when the opening is made for the child tunnel. Nevertheless, there is a concentration of stresses around the opening and, in the case of the junctions on Crossrail, this required the addition of steel bar reinforcement.

This project featured a large number of SCL junctions with a wide range of aspect ratios (of the “child” tunnel in comparison to the “parent” tunnel). The sensitive and complex urban environment of the project led to the extensive use of numerical modelling in the design process, inter alia to demonstrate that the impact on third parties could be managed safely (Goit et al., 2011). Rather than designing each individual junction with a 3D numerical model, as noted earlier, the design team performed a parametric study in 3D from which a set of design charts was derived to convert the results from 2D analyses of the parent tunnels into the concentrated stress values around the junctions. Typically each of the 5 mined stations on Crossrail has around 25 junctions so this approach saved a considerable amount of time on the design programme.

The axis level of the tunnels at Liverpool Street Station lies about 30 m below the ground surface and the tunnels were almost entirely excavated in the highly overconsolidated strata of the London clay. The invert of CH5 dips into the overconsolidated Upper Mottled Bed clay stratum of the Lambeth Group. The general geology of this area is described in more detail in Goit et al., 2011.

CH5 is roughly circular with an external diameter of about 11.75 m, which is the same as the platform tunnels. The cross-passages have an external diameter of 5.21 m for the pilot excavation and 7.09 m for the final (enlarged) cross-section – see Fig. 5. Hence the aspect ratios of the openings in CH5 are 0.49 and 0.68 for the pilot and enlargement respectively, based on the nominal centrelines of the lining cross-section.

The lining of the cross-passages is 250 mm thick and made of steel fibre reinforced sprayed concrete (SFRS). The primary lining of the concourse tunnel at CH5 is 400 mm thick and also made of SFRS. This was strengthened with an additional 400 mm thickening layer of SFRS with steel bar reinforcement, thus doubling the thickness of the primary

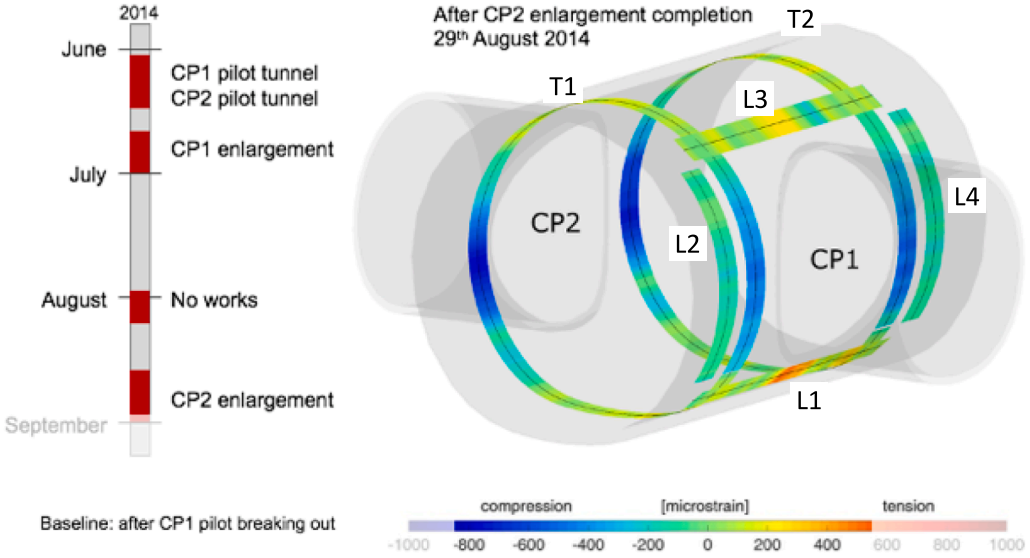

Fig. 4. Contour plot of the change in strain measured from the embedded DFOS cables after both cross-passages had been completed, along with the timeline for construction.

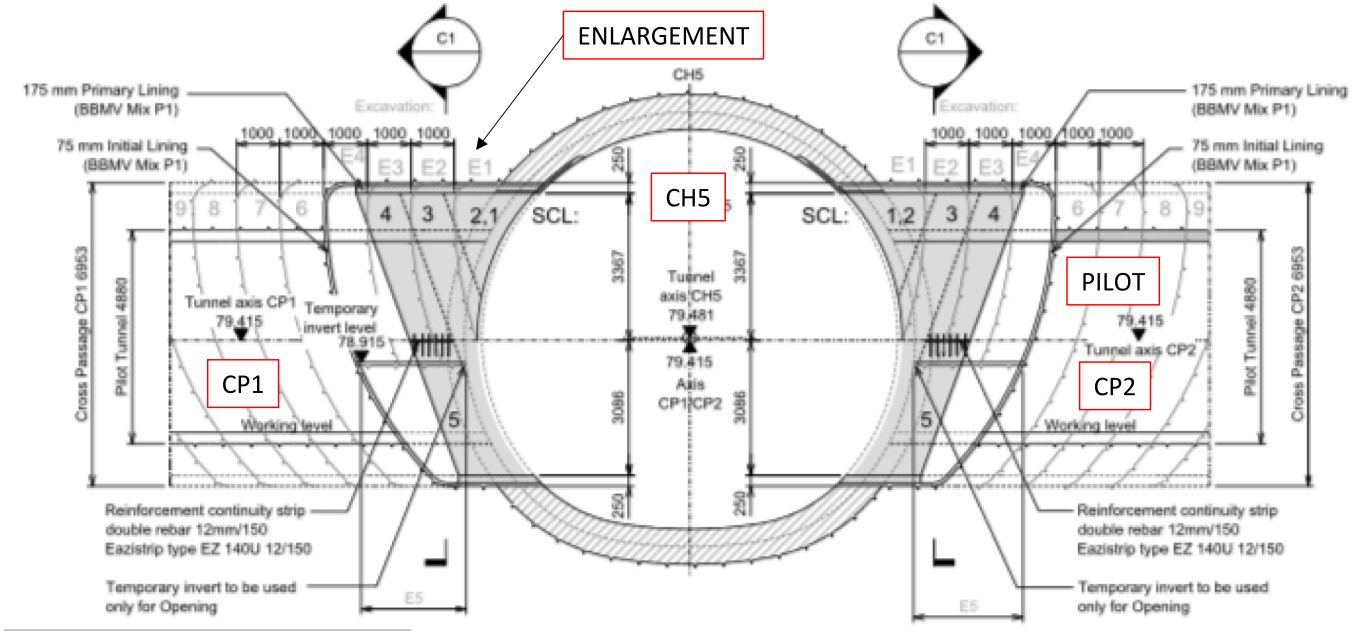

Fig. 5. Excavation sequence design drawing for the cross passages from CH5, showing each advance.

lining from 400 mm to 800 mm in total (see Fig. 6). The design specified that this thickening had to extend a minimum of 3.5 m (half a diameter of the child tunnel) on either side of the cross-passages. The bar reinforcement was typically 10 or 20 mm diameter bars at a spacing of 150 mm. This was installed inside the thickening layer since, for safety reasons, steel-fixing operatives were not permitted to work at the excavation face during the primary lining construction.

Following the excavation of the cross-passages, a sprayed waterproofing membrane and a secondary lining were installed over the (permanent) primary lining. However, since the DFOS monitoring was only carried out during the construction of the cross-passages, all the previous construction stages have not been considered in this study.

While the design approach worked well and the construction of the junctions progressed smoothly, there were still some questions about the heavy reinforcement around some junctions. The parametric study had predicted some patterns of load concentrations which did not match with the practical experience on similar SCL tunnelling projects – such as the Jubilee Line and Heathrow Express in London. These uncertainties were the motivation for using the DFOS monitoring data to re-examine some of the design assumptions adopted for these junctions. The field data provides a good opportunity to form a better understanding of the junction behaviour and possibly make useful recommendations for more efficient designs in the future.

In summary, one can highlight the following limitations in the original design:

- Linear elastic model for the lining in the numerical model;

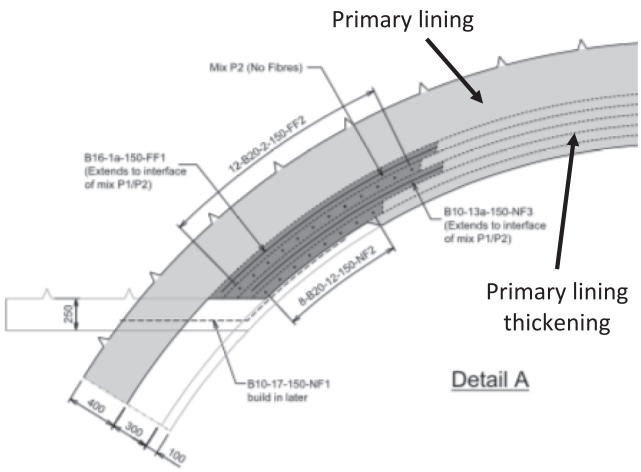

Fig. 6. Extract from reinforcement design drawing, showing the strengthening of the parent tunnel, CH5, above the junction on the centreline of the cross-passage.

- The numerical models showed some load patterns which are not believed to be realistic;
- The junction design was based on a parametric study which did not include any of the following items:
  - o Site specific adjacent structures
  - o Different excavation sequences
- The linings were thick and included significant bar reinforcement.

Nevertheless, the construction of the junctions in practice progressed very well.

4. Numerical modelling

4.1. General

For this study, a 3D numerical model of the junctions was built in FLAC3D. Fig. 7 shows a close-up of the mesh, illustrating the full extent of the tunnelled sections. The total mesh represents a block of ground 100 m long (along the axis of the cross-passages) by 23.5 m wide (along the centreline of the CH5) by 64.5 m high. The ground level is 34.5 m above the cross passage axis and the mesh extends 30 m below the axis of the tunnels. The boundaries of the mesh are located 3 to 4 times the diameter of the cross passage from those tunnels. The stratigraphy and position of the tunnels is based on the site specific data for Liverpool St station.

This is a quite sophisticated model and it could be said to represent the state-of-the-art in terms of numerical modelling of junctions in the commercial arena. The following features are noteworthy:

- A nonlinear elastoplastic constitutive model for the main strata, with depth varying properties – see section 4.2 and Goit et al (2011);
- Site specific ground properties, consistent with the original design inputs – see Table 1;
- Site specific profiles for the pore pressure, including the under-drainage of the London clay, and K0 – similar to those in Goit et al (2011);
- Detailed modelling of the excavation and lining sequence for the cross-passages, in line with the actual construction sequence – CP1Pilot, CP2 Pilot, CP1 & CP2 – see Fig. 5;
- One set of structural elements represents the two layers of the parent tunnel linings – the primary and the thickening layers. The thickness of the elements is changed after the parent tunnels have been built, before the openings are made;

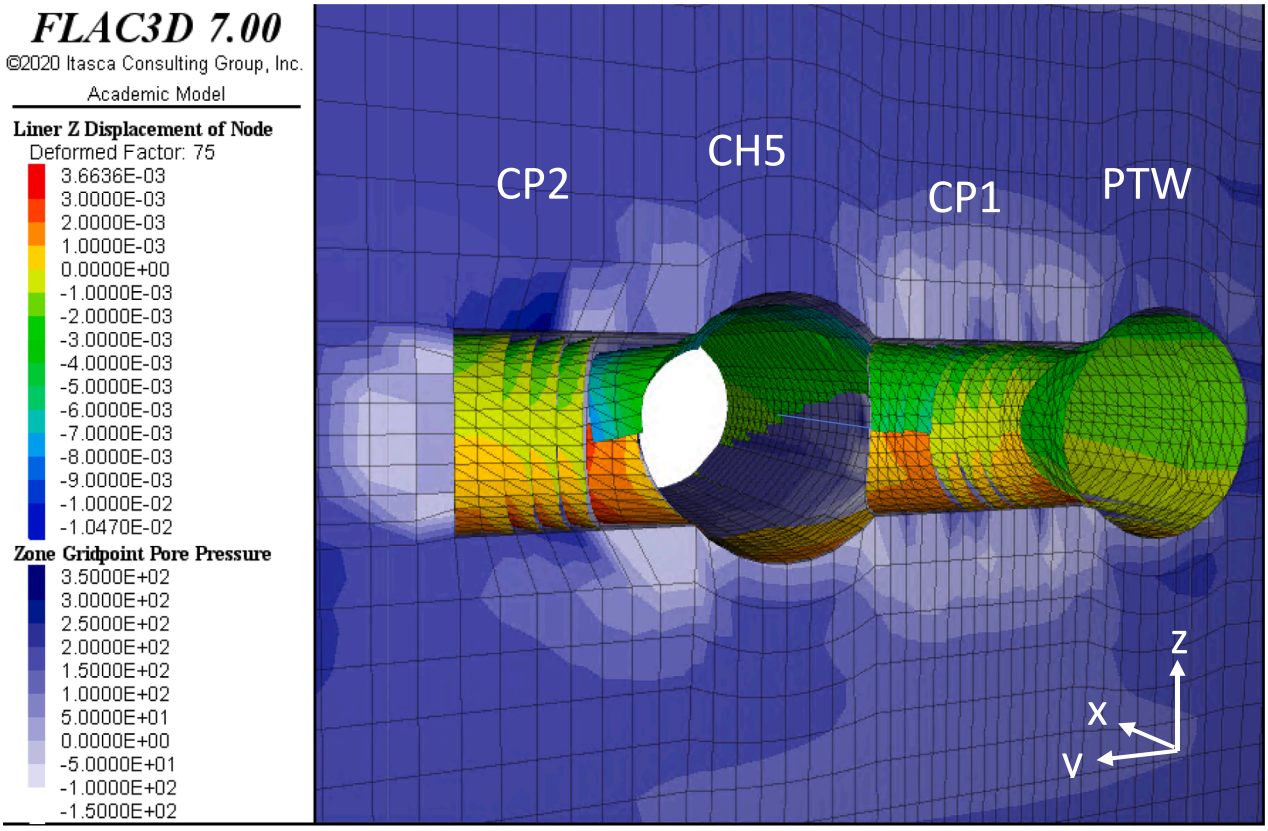

Fig. 7. A close up of the FLAC3D model, showing the pore pressure distribution in the ground, the contours of vertical displacement of the lining and the distorted shape of the linings, magnified 100 times.

Table 1
Ground properties.

Soil stratum (MLGH = mid Lambeth Group Horizon)	Bottom level (Ground level = 114.0 m)	Unit Weight		Cohesion	Friction	Poisson's Ratio	Undrained Shear Strength
	-	**Wet**	**Dry**	-	-	-	-
	-	γ	γ'	c'	φ'	ν ν'	Cu
	mATD	kN/m^3	kN/m^3	kN/m^2	Degrees	-	kPa
Made Ground	107.0	20.0	16.5	0	25	0.3	24
River Terrace Deposits	105.5	20.0	17.0	0	38	0.3	–
London Clay [A3] Above 89mATD	98.0	20.0	15.5	10	22	0.1	70 + 11z*
London Clay [A3] Below 89mATD	87.5	20.0	15.5	10	22	0.1	120 + 5z*
London Clay [A2]	75.5	20.0	15.5	15	26	0.1	110 + 7z*
Lambeth Group Clay above MLGH	73.25	21.0	16.5	25	27	0.1	110 + 7z*
Lambeth Group Sand above MLGH	68.55	21.0	17.5	0	37	0.2	–
Lambeth Group Clay below MLGH	65.5	21.0	16.5	25	27	0.1	110 + 7z*
Upnor Formation	57.8	21.0	17.5	0	37	0.2	–

* z is depth below top of London Clay.

- More detailed modelling of the tunnel linings (see later), such as an ageing elastic stiffness for the linings.

While the modelling approach is generally consistent with the one used in the original design and it is intended to simulate the real situation closely, this model does still include a number of simplifications, as follows:

- A single layer of structural elements is used to model the lining of the parent tunnel which was formed of two layers of sprayed concrete –see section 4.3;
- Geometrical simplifications including:
  - o CH5 is assumed to be perfectly circular.
    - o CH5 is modelled as a straight tunnel whereas in reality, CH5 narrows either side of the thickening zone from 9.5 m to 7.1 m internal width – see Fig. 1.
    - o The entire length of the parent tunnels was thickened whereas in reality, a length of approximately 10 m either side of the opening was thickened.
- Limited adjacent structures
  - o Only the Westbound Platform Tunnel (PTW) is included whereas the real situation is more complex (see Fig. 1). The Moorgate shaft, the upper escalator barrel and the Eastbound Platform Tunnel were not modelled.
- Uncoupled linings
  - o Each excavation advance in the cross-passage is free to move independently of the other advances and the parent tunnel. This is to avoid adding additional restraint to ground movements and inducing what are believed to be unrealistic tensile stresses in the linings in the longitudinal direction.
- A simplified construction sequence of the parent tunnels
  - o A two-step relaxation process rather than excavating the tunnels step by step. The relaxation procedure reduced the initial stresses from 100 to 40 % and then the lining was installed – as adopted in the original design.

4.2. Modelling of the ground

All the strata except the Made Ground are modelled with a nonlinear elasto-plastic model, which incorporates a modified Jardine model to replicate the variation in elastic stiffness with strain. The Made Ground was modelled as linear elastic perfectly plastic. Full details of the small strain stiffness model can be found in Goit et al (2011). This is the same approach that was used in the original design with the input values for the Liverpool Street Station area.

The strain measurements were taken in the immediate time period around the construction. Hence, the results presented here only consider short-term behaviour of the ground, (i.e. undrained behaviour for the clay layers and drained behaviour for the non-clay strata).

4.3. Modelling of the lining

A common feature of the numerical modelling of SCL tunnels is the use of elastic structural elements (Thomas, 2003 & Thomas, 2019). This simplification is often justified on the grounds that in civil engineering the normal factors of safety limit the stresses within a tunnel lining to well beyond the compressive limit. However, at stresses of above about 40 % of the uniaxial compressive strength, concrete exhibits a nonlinear elastic response (Thomas, 2019). The results presented here are from linear elastic models only but in a separate part of this study nonlinear elastic models were used. This will be presented in a subsequent paper.

Besides the obvious limitations in terms of compressive behaviour, one should note that this also assumes that the behaviour in tension is the same as in compression. Tunnel linings are designed to work primarily in compression and on Crossrail considerable care was taken to minimise any bending in the lining so that fibre reinforcement alone could be used (Thomas, 2021). Nevertheless, there are some cases – such as junctions – where larger bending moments were predicted and hence additional bar reinforcement was added – as described in section 3. Given the factors of safety used, the lining should be operating within the Serviceability Limit State and, although parts of the lining may experience some tension due to bending (on either the inner or outer faces), the extent of cracking should be very limited. Both bar and fibre reinforced concrete behave linear elastically in tension until the tensile strength of the concrete is exceeded. In this context, it is reasonable to assume that most of the lining remains in the elastic region of concrete behaviour in tension.

An approach that is sometimes used is to model the lining with zones instead of structural elements. This enables a wider range of constitutive models to be used. However, two major drawbacks appear. First, the zones (which are constant strain elements) behave in an inherently stiffer manner than the structural elements. At least 6 zones are needed across the thickness of the lining for the error in bending moment to be reduced to less than 5 %. This produces significant problems with mesh discretization and construction for one tunnel. This becomes unfeasible for the geometry of a junction. Secondly, one has to manually calculate the axial forces and bending moments from the stresses in the zones. Again this would become much more complicated for a junction model. The latest version of Flac3D, which was released after this study, now offers a wide range of constitutive models for structural elements.

As mentioned earlier, one set of structural elements represents the two layers of the parent tunnel linings. This is a simplification which naturally has some disadvantages but it also has some significant advantages. In real tunnel, there are two distinct layers – one only reinforced with fibres and the other with both fibres and steel bars – which are designed to act in concert. Initially all the load accumulated, during the construction of CH5 and the adjacent platform tunnels several months earlier (see Fig. 1), is contained within the primary layer and the thickening is unstressed – except for any stresses due to self-weight,

shrinkage and thermal effects. As the cross-passages are built, the additional load will be shared between the two parts of the lining. If one assumes elastic superposition and a fully composite action, this change in load should result in an even change in strain across the whole section from which the induced axial force and bending moment for the lining could be computed. This is done automatically by Flac3D for a single layer of elements, using the current parameters for the lining, since it works on an incremental basis. The original load in the lining is not lost since force equilibrium must be maintained at all nodal points.

Alternatively, if one uses two layers of structural elements with an interface element in between, the new axial force can be easily calculated as the sum of the axial forces in each layer. The bending moment is much more problematic to interpret because Flac3D reports the bending moments for each layer separately. These cannot be simply added. Since the design assumes that both layers act as a composite, the bending moment of the total section is essential for the check on the capacity of the lining.

Obviously by using one layer of elements, it is not possible to track how the stress and strain change across the two layers of the lining. However interesting this would be to examine, there is no monitoring data on the distribution within the thickness of the lining – see section 2 – and therefore nothing to compare those results with.

On the positive side, the results are extracted from the structural elements on their centreline – i.e. the mid-point of the thickness of the lining. This coincides with the actual location of the DFOS cables – see section 2. Furthermore, this method of modelling the lining is consistent with the approach used in the original design, which eases the comparison with that design. Hence, considering the merits and disadvantages of each method, it was decided to use the single layer of structural elements.

4.4. Runs of numerical models

Table 1 contains a list of the simulations that will be discussed in this paper, with notes to explain the main features. Further models have also been run to investigate aspects such as the simulation of for each excavation step and the nonlinear behaviour of concrete. The results from these will be presented in future publications.

The Base Case model, Et, can be characterized as “a designer’s best estimate”; in other words, site specific data has been used for both the ground and the lining. The parameters have not been adjusted to obtain a better match with the monitoring data. The excavation sequence has been modelled in detail in the area of most interest – namely, the cross passage excavation. The overall sequence was the CP1 pilot, then CP2 pilot, CP1 enlargement and finally CP2 enlargement. This work focuses on the changes due to forming the junctions which are arguably to a large degree independent from the initial stress state in the parent tunnel. As noted earlier, the parent tunnel was completed months before the cross-passages were built. One reason for omitting some of the adjacent structures is that this makes the effect of varying features within this model much clearer, since secondary effects from the interaction with the adjacent structures will not obscure the picture of behaviour.

5. Results of the numerical modelling – Base case

This section will focus on the base case run (Et) with the results of the other runs discussed in section 6. In general, the pattern of behaviour in the numerical models – in terms of the re-distribution of stresses and the movements in the ground and the linings, and the movements in both - is consistent with what would be expected (e.g. after Jones, 2007; Thomas, 2019; Chortis & Kavvadas, 2020). The use of a nonlinear elasto-plastic model for the ground leads to localised movements and a limited extent of yielding in the ground. Similarly, the changes in pore pressure occur mainly within 0.5 diameters of the extrados of the tunnels (see Fig. 7).

5.1. Volume loss

Volume loss is a relatively coarse parameter but it does give an indication of the performance of a tunnel. A well-constructed SCL tunnel would result in a volume loss of 0.50 to 1.00 % (Thomas et al., 1998) and the original (2D) design models predicted values in this range. The actual volume loss of the tunnelling work at Liverpool St station is not known. There were significant amounts of compensation grouting undertaken during construction, which makes the calculation of volume losses very challenging. Hill & Staerk (2016) calculated volume losses of between 0.49 and 0.55 % for similar SCL tunnels at the Whitechapel Crossrail station using short-term settlement curves. Although those tunnels are slightly shallower, it is reasonable to assume that the volume loss at Liverpool St station was similar since the two stations share many common characteristics, ranging from similar geology to the fact that the same contractor built both sets of tunnels with the same methods. Similarly, Gakis et al (2016) reported a volume loss of 0.4 to 0.5 % for the enlargement of the TBM pilot tunnel to the full platform tunnel cross-section at Crossrail Farringdon station.

Fig. 8 shows the volume loss for the construction of the parent tunnels and the incremental volume loss of the construction of the cross-passages. The simulations resulted in volume losses which match well with the expected range, although the volume loss for the parent tunnels is less than 0.40 %. This low value could imply that the initial lining loads are overestimated. In fact the axial force was within about 5 % of the axial force predicted in the original (2D) models for these tunnels.

Most models show very similar values with a tendency for the first break-out to result in a higher volume loss than both the subsequent stages and the parent tunnel construction. By the end of the cross passage construction, corresponding volume loss is low, ranging from 0.41 to 0.47 %. Thomas et al (1998) reported similar, smaller volume losses for the later enlargement of tunnels, compared to the construction of the first tunnels.

The volume loss was initially higher for CP1 (excavated between the parent tunnels in the model) than for CP2 (excavated in less disturbed ground in the model). By the time the cross passages are complete, the volume loss for both cross passages had settled at a value which is slightly higher than that for the original parent tunnel construction (~0.44 %).

5.2. Deformations of the lining

Unfortunately, there is very little information about the lining deformations from the construction records, even though convergence monitoring points were installed in CH5 and the cross-passages. The incomplete data that has been obtained from the project archives is in line with more comprehensive studies of lining deformations in Crossrail SCL tunnels (Staerk et al., 2016). Fig. 9 shows data from a single monitoring point in the crown on the centreline and an array which was 2.5 m from the edge of the opening.

Arasteh (2018) presented values for lining movements at junctions at Farringdon, which ranged from 5 to 11 mm of vertical movement in the crown points. These junctions are at a shallower depth (about 27 m) than CH5 (35 m deep). Therefore, one. One might expect the actual movements at Liverpool Street station to be slightly larger. Stark & Jimenez (2016) report similar values for junctions at Whitechapel (which is at a similar depth to Farringdon). They also noted that the measured convergence was less than that predicted in the design. The green and red warning trigger values for vertical displacement were 10 mm and 20 mm, respectively.

Fig. 9 shows the increments in vertical movements due to the openings from various models, along with the data from CH5 and Farringdon station. The values have been magnified to show the distorted shape more clearly. Two sections are presented – on the centre line of the junction with the cross passages and 0.5 m from the edge of the opening. The predictions lie in the same range as the measured values. The

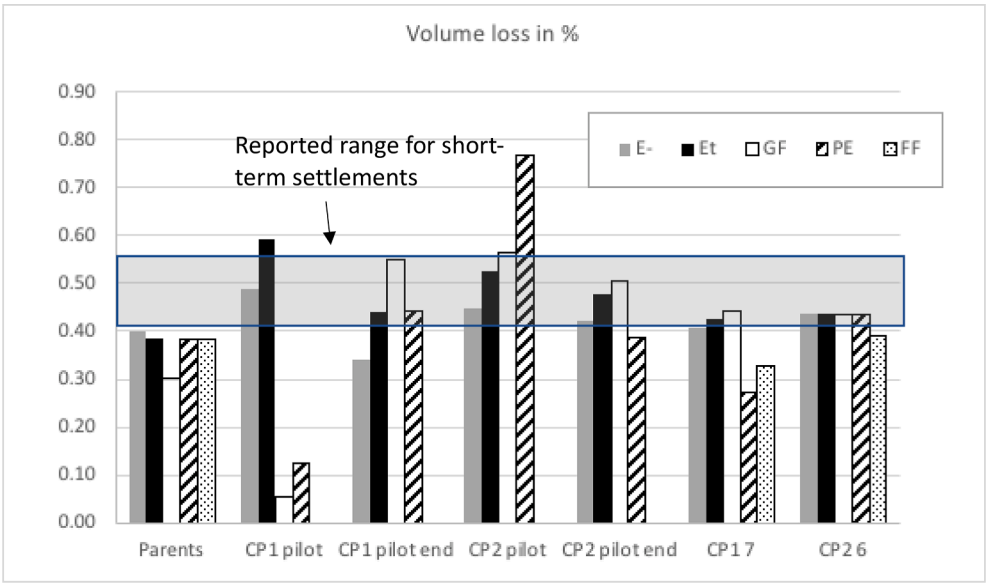

Fig. 8. Predicted volume losses from the numerical models with measured values.

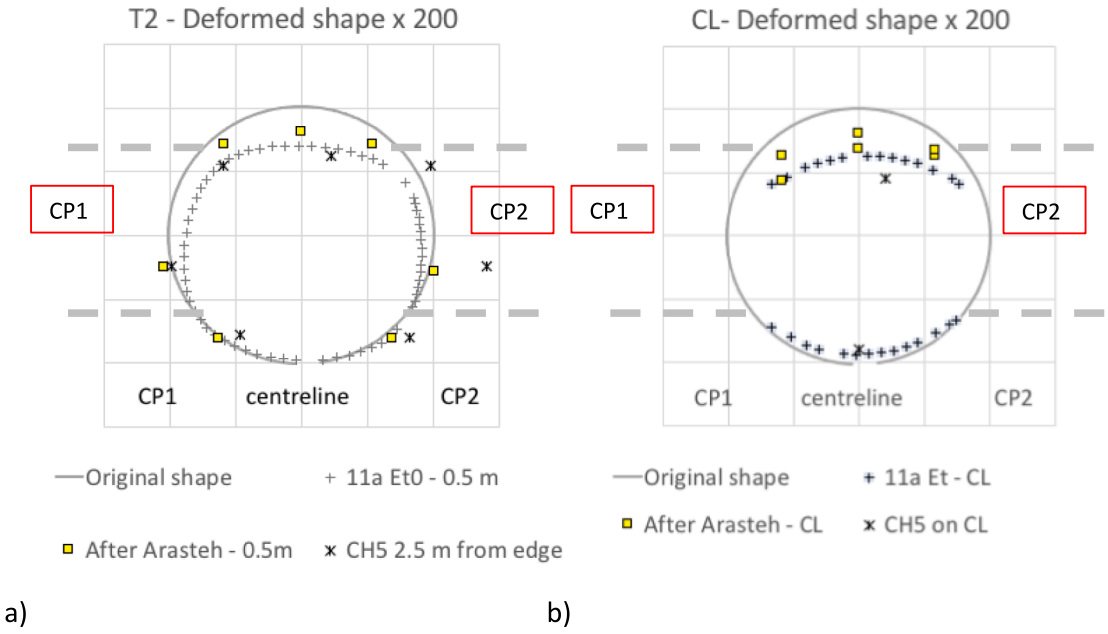

Fig. 9. Predicted displacement of parent lining a) at 0.5 m from the edge of the opening and b) on the centreline of the junction (magnified by 200x), along with measured data.

models predict a slightly asymmetric deformed shape for the lining of CH5 because on one side (CP1) in the model there is an adjacent tunnel – PTW – while on the other side there is not. However, the measured data from CH5 shows a more pronounced asymmetry. These points are also slightly further from the edge of the opening (2.5 m away) and they may have been affected by the asymmetric arrangement of the real adjacent tunnels, which are closer on side of CP2.

5.3. Strains in the lining

A full account of the results of the DFOS monitoring can be found in de Battista et al (2015). As shown in Fig. 4, the measured strains indicated elevated compressive strains adjacent to the cross-passage openings, particularly along the lines closest to the opening. The measurements also showed that, due to the opening, the strains decreased in the longitudinal direction above and below the centreline of the opening, particularly below the opening. These are strains along the centreline of the lining cross-section, since the FO sensor cables were installed between the primary lining and the thickening layer. Hence, they reflect approximately the average stress in the lining.

In broad terms, the base case numerical model agrees well with the pattern of strain measurements adjacent to the openings. Fig. 10 shows the strains at different stages in the circumferential loop that was located 0.5 m away from the edge of the cross-passages, with the angle measured from 0° at the crown to 180° at the invert. The magnitude of the strain measured at the final stage close to the opening is substantially higher than the strain predicted by the model but the magnitudes agree better where the lining is less heavily loaded, for example at 2 m from the

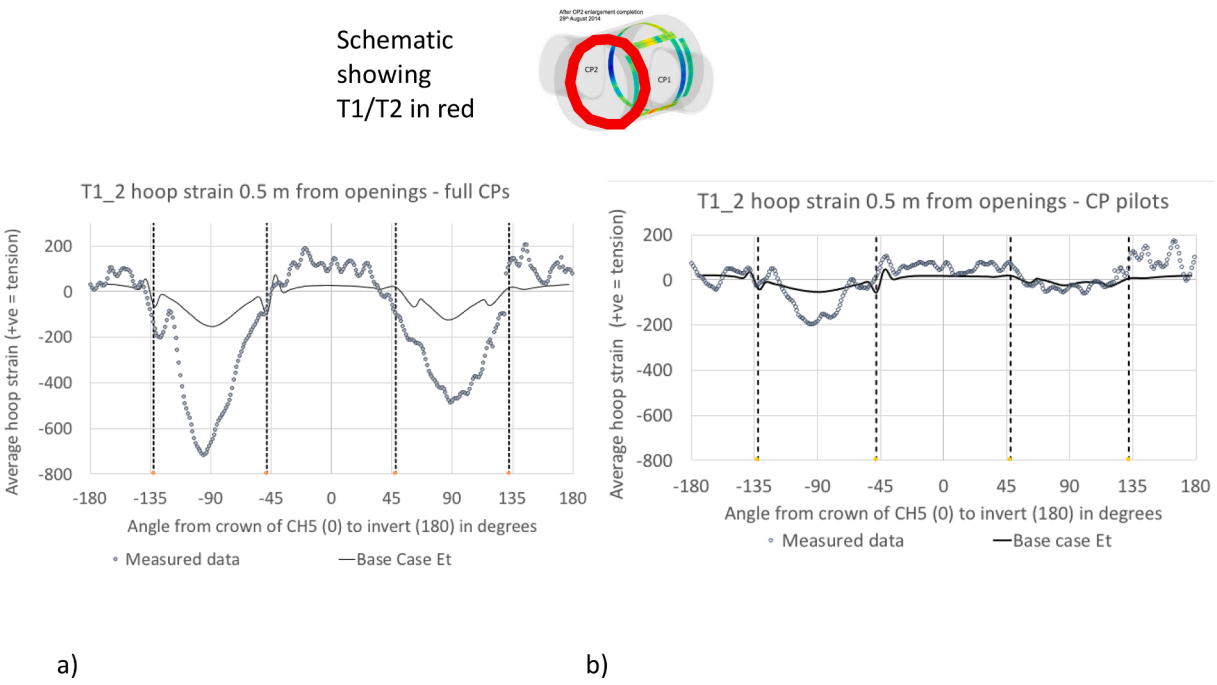

Fig. 10. Average predicted strain measurements in loop T1/T2, 0.5 m from the edge of the opening: a) after the completion of both CP pilot tunnels & b) after both enlargements with measured values.

opening (see Fig. 11) or at early excavation stages (see Fig. 10 a).

In contrast, there is less good agreement in the longitudinal strain above and below the opening (see Fig. 12). While the predicted strains are of the same magnitude, the pattern does not agree well. During construction, the predicted longitudinal compression forces increase at the junction, in particular in the crown of the parent tunnel. The estimates of average strain (calculated from the models' nodal displacements) are consistent with these forces. In contrast, both longitudinal FO cables showed show an increasing tensile change in strain. The cable in the invert, L1, showed particularly high strains, up to 450 με, which could be approaching the tensile limit of the concrete.

At larger aspect ratios of an opening, the area between the openings begins to function more like a flat plate spanning longitudinally under a semi-uniform load from the ground. This would tend to induce sagging which leads to a compressive change of strain (and stress) on the outer face of the lining and a tensile change of strain on the inner face (see Fig. 13). This could be one explanation for the tensile changes in strain measured. The exact explanation for the discrepancy remains unclear and deserves further investigation. It is possible that the other locations, either side of the opening, were less affected by some of the above because they experience a more uniform compression and less bending.

5.4. CH5 lining loads

Fig. 14 and Fig. 15 show lining loads in the area beside the tunnel opening as a representative selection of results. This is for a line of

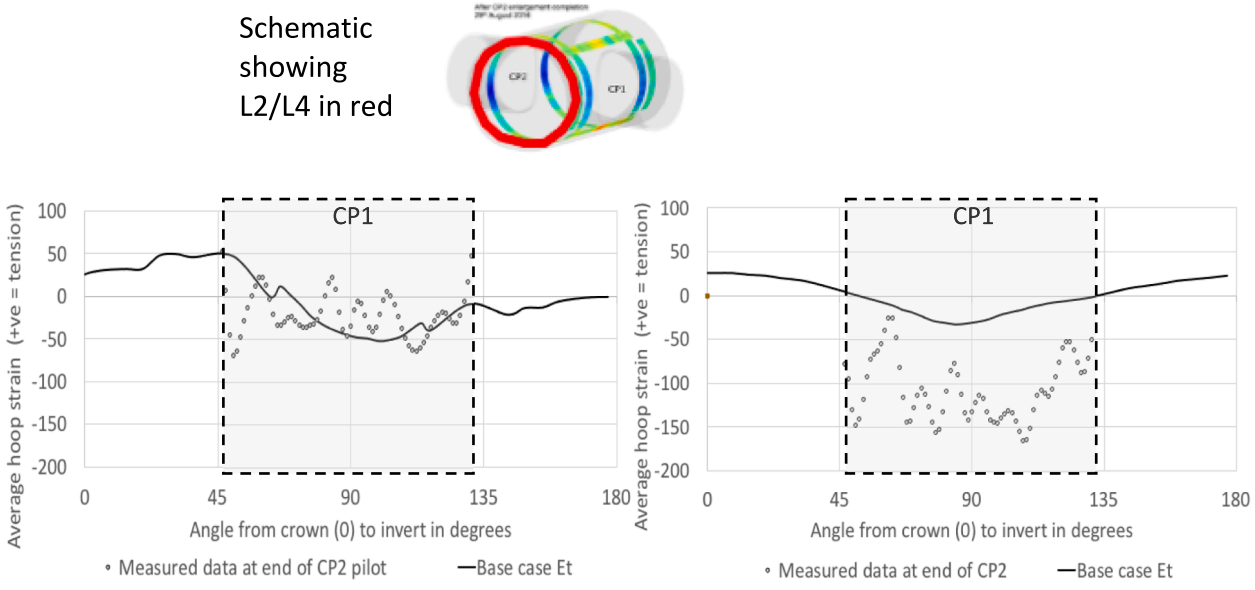

Fig. 11. Average predicted strain measurements in line L2/L4, 2.0 m from the edge of the opening with measured values.

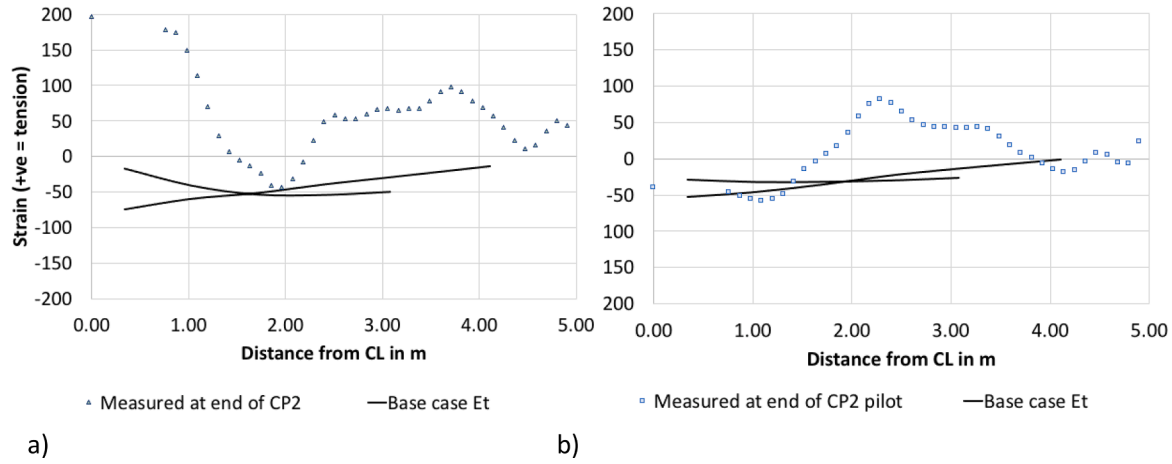

Fig. 12. Average predicted strain measurements in line L3, 0.5 m above the crown of the opening: a) after the end of CP2 pilot b) after the end of CP2 enlargement with measured values.

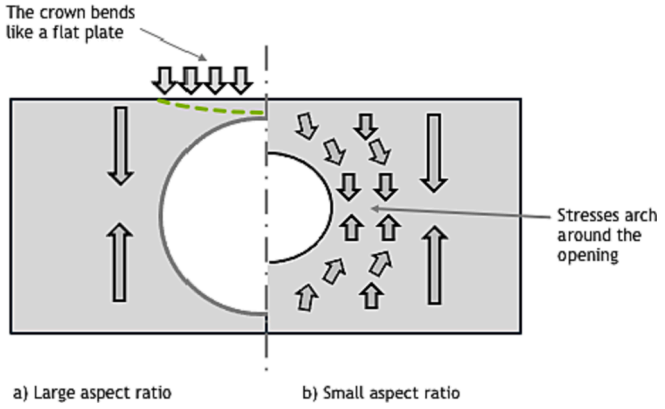

Fig. 13. Schematic of the different modes of behaviour of tunnel linings at openings with large and small aspect ratios.

sampling points at the axis level of CH5, running from the edge of the opening for CP1. The results are presented for the final stage when all the cross passage construction is complete.

For ease of comparison, the hoop load (axial force) results have been normalised according to the "base hoop load" (Ny) in CH5 before breakout in the case of Fig. 14, while Fig. 15 shows the increment in hoop bending moment due to the openings. This is only one of the governing points in the design of a junction. However, it tends to be the governing case for compressive loads. The figures show the results at the end of construction of the two cross-passages. The situation at the intermediate stages is similar. The pattern is consistent with the change in strains which show big increases in compressive strains at the axis level, beside the openings.

Fig. 14a and Fig. 15a include results from the same area adjacent to the opening for CP2, on the other side of the parent tunnel, CH5. The results appear to be almost identical.

Considering the loads at the axis adjacent to CP1, the concentration in axial (hoop) loads is similar in all models. There is a sharp concentration in the hoop force beside the opening as expected – see Fig. 2. The concentration in loads increases as the construction proceeds. In Fig. 14a, the loads after all the cross passage construction are compared with the analytical solution for a "hole in an elastic plate" by Kirsch – which is commonly used to estimate this concentration in design (Thomas, 2019). The figure also includes some pressure cell measurements from Heathrow Express (Jones, 2007) which is a similar tunnel in London clay. There is no field data on bending moments to compare with the predictions in Fig. 15.

Fig. 16 shows the pattern of predicted hoop forces along the line of the strain measurements in loop T1/T2, 0.5 m from the edge of the opening. The pattern of the concentration of axial force (hoop force) matches the pattern implied by the strain measurements. Because of the ageing and nonlinear behaviour of the sprayed concrete, it is difficult to compare forces (or stresses) with strains in general. In this case, there was relatively little change in the stiffness of CH5′s lining while the increments in load due to the cross-passages were added. If one back-calculates the effective elastic modulus of the concrete from the peak measured strain and peak predicted hoop load, this appears to be around 7.5 GPa, which is only 20 % of the instantaneous elastic modulus measured on samples of the concrete at the construction site (see Fig. 16).

Fig. 16 shows results for both the Base case (Et) and Design case (E-). The results from the other models showed very similar patterns.

5.5. CP lining loads

The lining loads for the cross passages will be examined in detail in the next phase of work so they will not be discussed further here, except to note that the whole of the cross-passage linings appear to be in tension in the longitudinal direction in all of the model cases. Typically this tension was more than 200 kN, in comparison with a capacity of about 165 kN for the steel fibre reinforced sprayed concrete in direct tension. This effect was observed in the original design calculations and other similar studies (e.g. Kropik, 1994; Hafez, 1995; Thomas, 2003; Jones, 2007). However, this is at odds with the anecdotal evidence from tunnelling sites, as tension cracking due to longitudinal forces has not been reported.

5.6. Summary of base case modelling

Generally speaking, it is uncommon for complex numerical models to agree well with monitoring results in all aspects. The models tend to be geared towards simulating one aspect of the case and hence the agreement is good in that specific aspect but weaker in other areas.

In this case, there appears to be a broad agreement both in terms of ground and lining behaviour, even allowing for the fact there are only few site specific measurements to compare with. The pattern and magnitude of the changes in ground movements and ground stresses matched what would be expected in SCL tunnels like these from similar studies such van der Berg, 1999; Thomas, 2003 or Jones, 2007 (e.g. Fig. 7, Fig. 9 and Fig. 14). The volume loss aligned with the reported range for Crossrail SCL tunnels (e.g. Hill & Staerk, 2016; Gakis et al.,

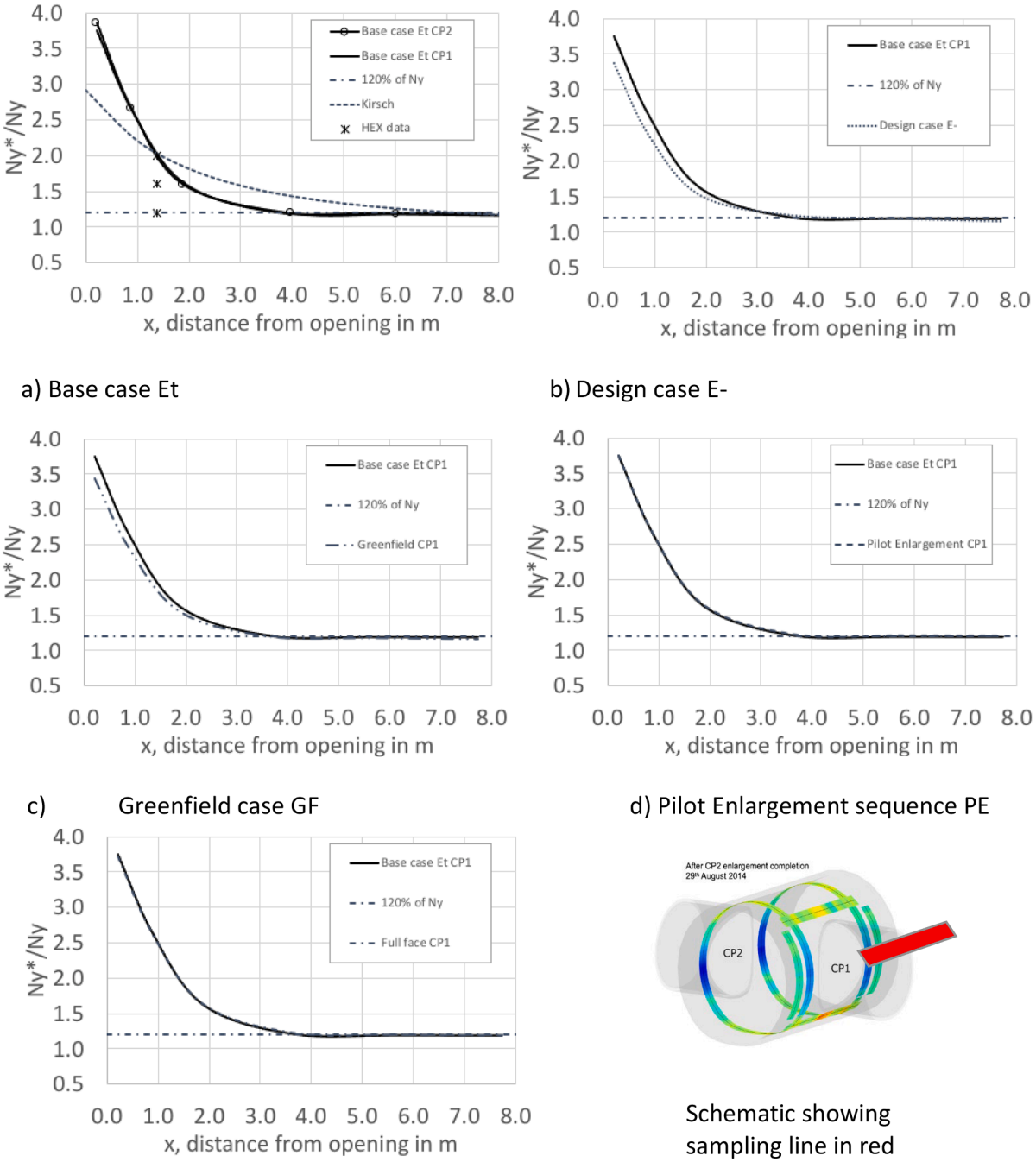

Fig. 14. Predicted normalized hoop force in CH5 at its axis level vs distance from the edge of the opening.

2016). The behaviour of the lining matched well – e.g. in terms of strains and deformations, as described in sections 5.2 and 5.3. The predicted lining loads similarly exhibit the behaviour predicted in the design (and data from the Heathrow Express project) and lie within a similar range, except that the bending moments tend to higher than expected. It should be emphasized that these models have not be specifically tuned to match any particular parameter. Instead they have adopted the general approach used in the design and the site specific input data.

That said, several areas remain which could be improved:

(a) The lining above and below the opening – see section 5.3

(b) Longitudinal tension in the lining of the child tunnel – see section 5.5

Further work is focussing on the constitutive behaviour of the concrete lining and the procedures in the model for simulating the excavation and lining process.

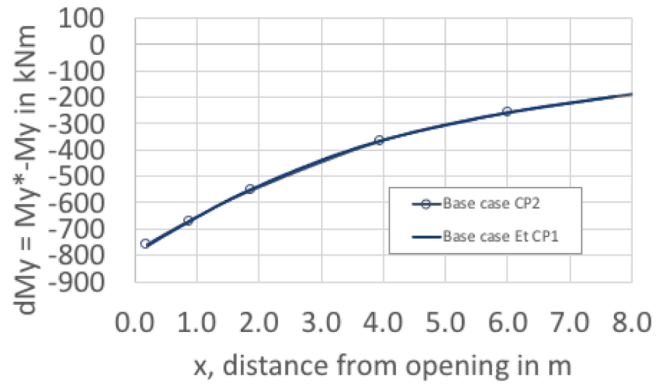

a) Base case Et

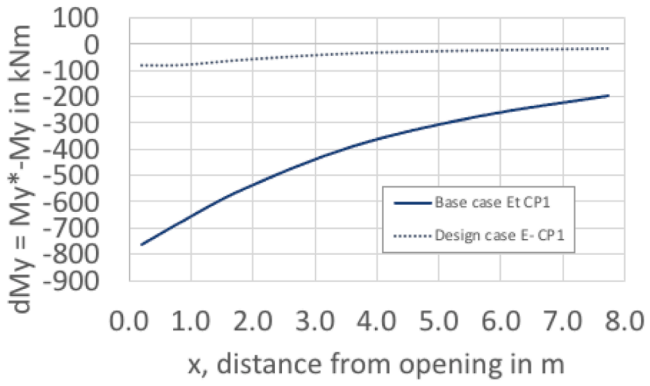

b) Design case E-

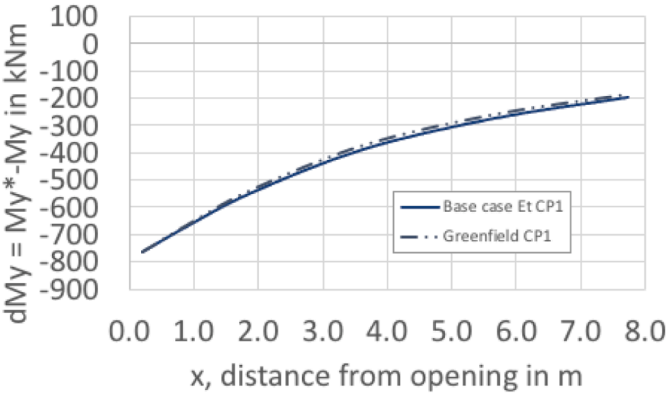

c) Greenfield case GF

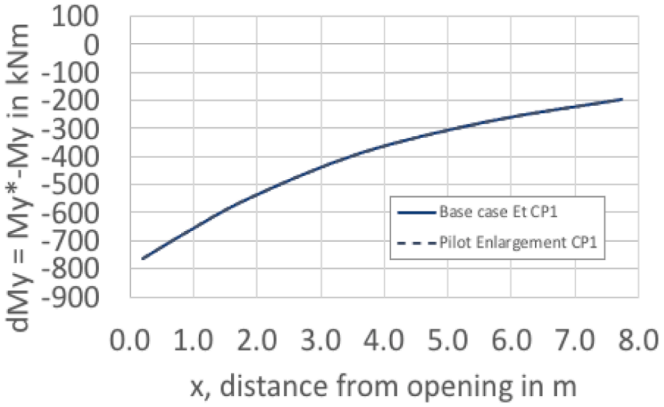

d) Pilot Enlargement sequence PE

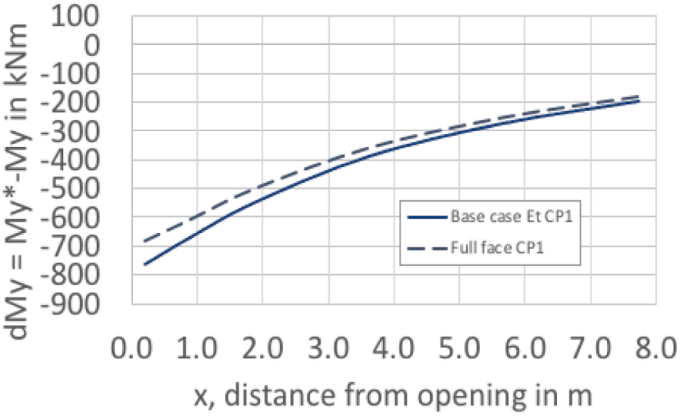

e) Full face sequence FF

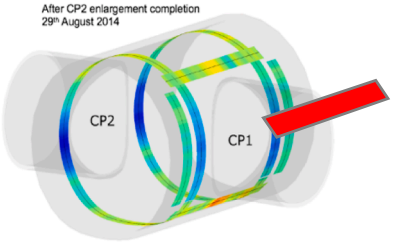

Schematic showing sampling line in red

Fig. 15. Predicted hoop moment increment in CH5 at its axis level vs distance from the edge of the opening.

6. Discussion

6.1. Lining stiffness

As noted above, the "design case" (E-) model is substantially softer in bending because it is both thinner (400 mm vs 800 mm) and its elastic modulus is 60 % of the base case model (Et). Consequently, the lining is much softer in bending, so the lining movements are higher. The lining deformations are substantially higher (see Table 2). For ease of comparison, Table 2 only contains a selection of data at the location of convergence monitoring points in the crown of CH5 on the centreline of the opening (c.f Fig. 9b). The volume loss at the end of the cross-passage construction is also slightly higher (see Fig. 8). The hoop forces are about 10 % lower but the change in bending moments is much lower – only about 10 % of the change in the base case moments (see Fig. 15b). It is well known in the design of underground works that "stiffer" structures

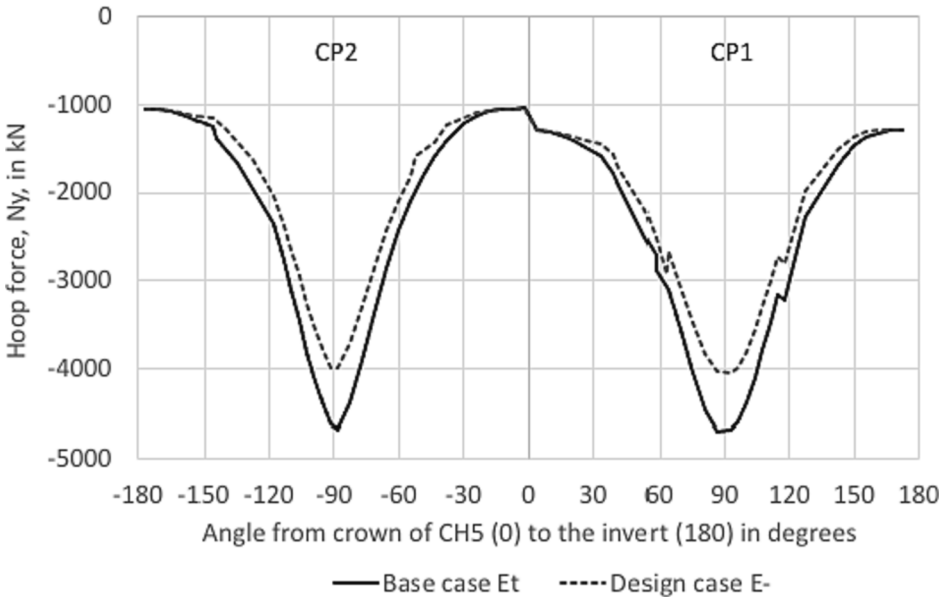

Fig. 16. Predicted hoop force in CH5 along the line of T1/T2, 0.5 m from the edge of the opening, after the completion of both CPs.

Table 2
Numerical modelling simulations.

ID	Description	Features of the simulation
10 E-	"design case"	A linear elastic model for the primary lining with a constant stiffness of 15 GPa. Only the primary lining of the parent is modelled (400 mm thick). An ageing elastic model is used for the cross passages. This model mirrors the original design analyses.
11a Et	Base Case	An ageing linear elastic lining model with a 28 day stiffness of 25.8 GPa. Primary lining and thickening modelled with a single layer of structural elements, as described above (see also Section 5) – totalling 800 mm thick.
13a PE	CP1 pilot-enlargement; CP2 pilot-enlargement	Based on the base case but with a different order of construction. The tunnelling is completed at CP1 before CP2 is started (Section 6.2).
13c FF	Full face sequence	Based on the base case but the full cross-section of the cross-passages is built without a pilot. The initial break-out sequence with the Top Heading and then Invert is used (Section 6.2).
11b GF	Greenfield	Based on Et but the PTW tunnel is omitted from the model (Section 6.3) – i.e. no adjacent structures.

attract higher bending moments.

Ageing (of the parent tunnel) will not be so relevant for the case of a junction where the concrete is already close to 28 days old before the openings are made. A model with an age-independent stiffness could be used for the parent.

However, the linear elastic models do not appear to be able to replicate the localised pattern of strains which is visible in the measured data (see Table 3 and Fig. 18), although there is a better match at the earlier stage when only the pilots have been built (see Fig. 17). The "softer" model predicts slightly higher strains than the base case in the most heavily loaded sections and similar values in less loaded areas. This suggests that models which simulate the nonlinear behaviour of concrete are worth investigating since these would tend to result in more localised and higher strains in more heavily loaded areas, where the nonlinearity leads to a lower stiffness.

Table 3
Vertical displacement in mm of parent lining vs measured data.

Monitoring point \ Model	M2 Left shoulder*	M1 Crown	M3 Right shoulder
Arasteh (2018) average values	−8.5	−6.5	−5.5
CH5	–	–	−14.0
Design case, E-	−14.2	−13.8	−14.1
Base case, Et	−8.2	−9.4	−7.6
CP1/CP2 sequence, PE	−7.4	−5.4	−6.3
Full face, FF	−7.0	−5.4	−5.8
Greenfield, GF	−6.2	−7.0	−6.3

* on the side of CP1 which is the first cross passage to be built.

6.2. *Excavation sequence*

The actual construction sequence comprised the construction of a 4.71 m internal diameter (ID) pilot tunnel for CP1, followed by a similar pilot tunnel for CP2. Then CP1 was enlarged to the full cross section with an ID of 6.59 m and finally CP2 was enlarged to the same size. When each tunnel was started, the first section of about 3 m was built using a Top Heading and Invert sequence, while the remainder was full face excavation. A number of other excavation sequences were simulated in the numerical models to investigate the importance of this sequence:

- CP1/CP2 sequence - PE: CP1 pilot, CP1 enlargement, CP2 pilot, CP2 enlargement
- Full face excavation - FF: CP1 enlargement, CP2 enlargement - i.e. no pilot tunnels.

Because the sequences are different, it is difficult to compare the intermediate stages. However, the final situation can be assessed. As Fig. 14d and Fig. 15d show, the order of excavation does not appear to have any meaningful impact on the final hoop forces and moments. This matches with the findings of Chortis & Kavvadas (2020). Similarly, omitting the pilot tunnel does not appear to have any detrimental effect (see Fig. 14e and Fig. 15e). The strains at the final stage are identical to the base case model (see Fig. 18e). Omitting the pilot tunnel did result in the lowest volume loss (see Fig. 8) and lowest lining deformations (see Table 2). This may be due to the fact that the ground does not undergo successive processes of softening.

Overall, this implies that there is more freedom in the choice of

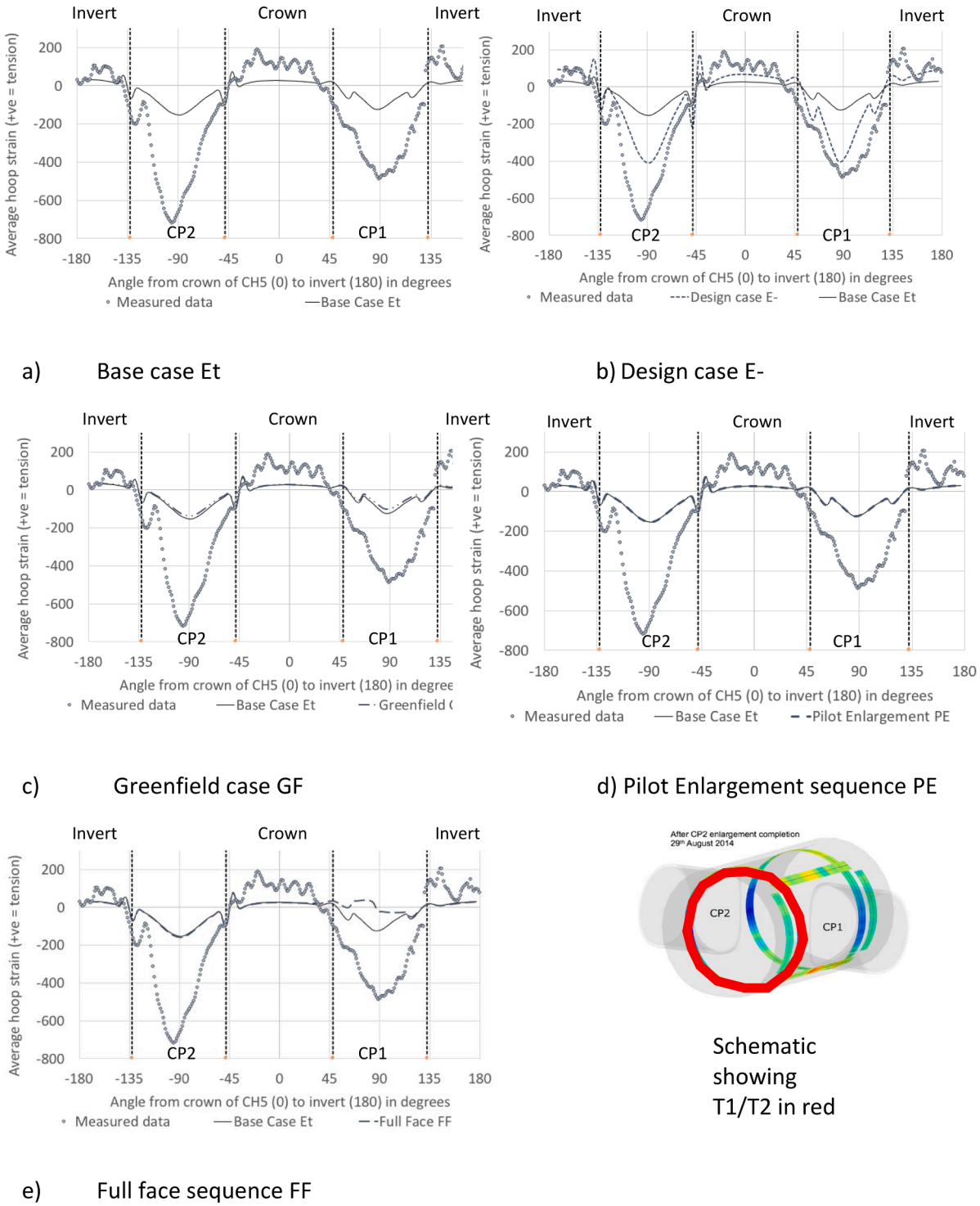

Fig. 18. Average predicted strain measurements in loop T1/T2, 0.5 m from the edge of the opening, after the completion of both CPs with measured values.

excavation sequence than the original design foresaw. For example, if the pilot tunnel could be omitted, roughly speaking this could cut the construction time in half. There would also be a substantial saving in materials that are used for the temporary lining of the pilot tunnels, which in turn reduces the carbon footprint and cost of these works. This assumes that there are no local reasons which prevent this, such as localised block instability in the face that this continuum model has not identified. Gakis et al (2016) came to a similar conclusion in relation to the order of the steps within the platform tunnel enlargement construction sequence for Crossrail Farringdon station.

6.3. *Adjacent structures*

As Fig. 1 shows, the studied junction was located in a complex part of the station with a number of new and old tunnels nearby. An obvious question to ask is how much these adjacent structures affect the stresses and strains in the junction. To assess this, the platform tunnel Westbound (PTW) was included in the basic mesh.

Fig. 18c shows that the model without PTW – the Greenfield (GF) case - generally predicts slightly lower strains. Considering the lining loads beside the opening, Fig. 14c shows that the hoop loads are also

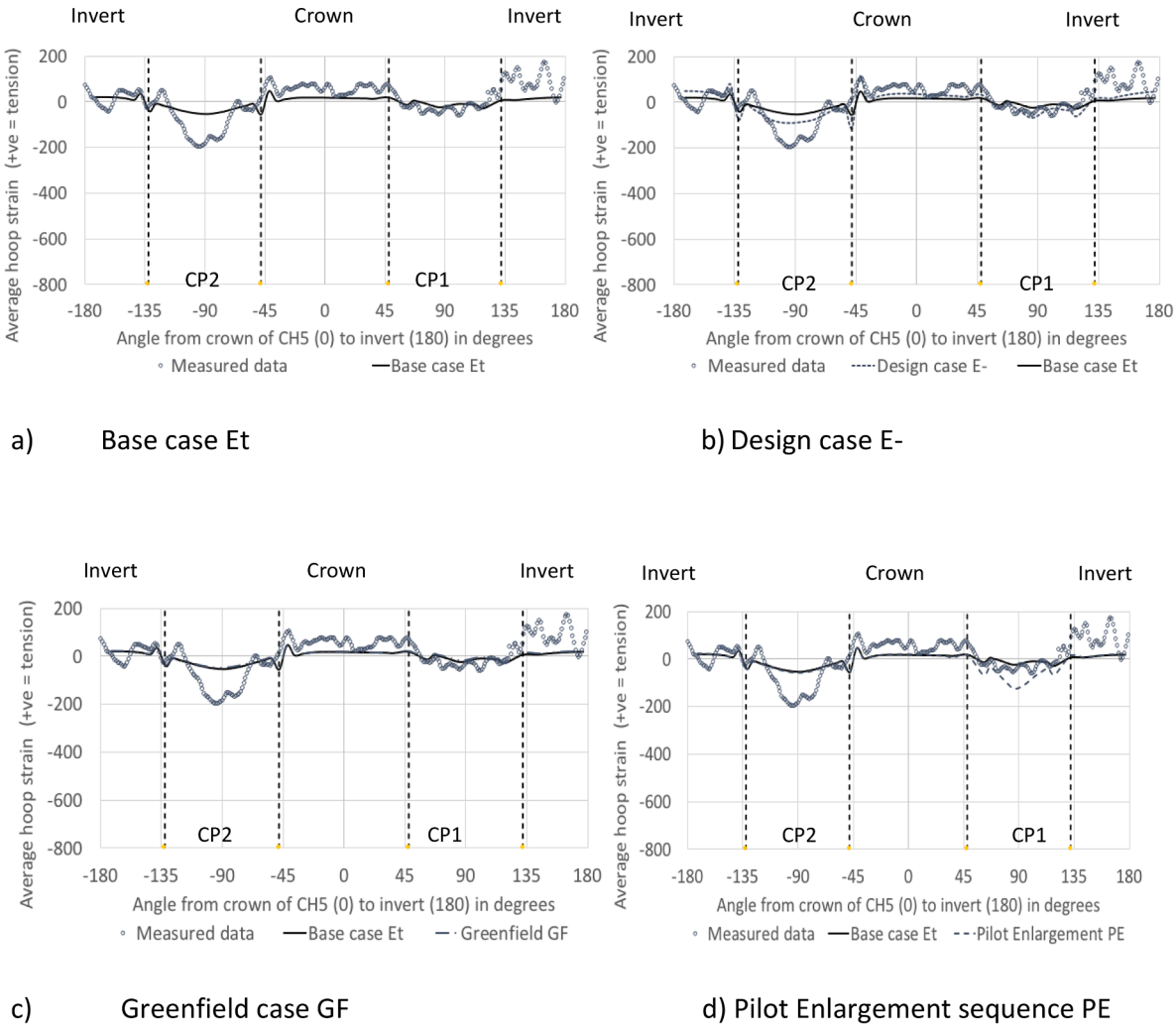

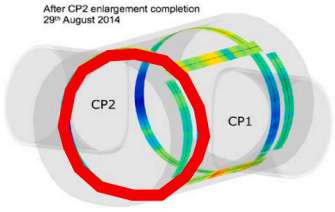

Schematic showing T1/T2 in red

Fig. 17. Average predicted strain measurements in loop T1/T2, 0.5 m from the edge of the opening, after the completion of both CP pilot tunnels with measured values.

lower if the adjacent tunnel is omitted. This is unsurprising since the clear separation between the tunnels is only about 7 m, approximately 2/3 of a tunnel diameter for CH5. At this spacing one would expect some interaction between the two parents tunnels (Thomas, 2019; Chortis & Kavvadas, 2020). This in turn would influence the junction behaviour negatively. CP1 will be excavated through ground that has been disturbed by both CH5 and PTW. However, the magnitude of the impact seems very small.

Nevertheless, where adjacent structures existing in close proximity (i.e. within less than 0.67 × the parent tunnel diameter), it would be best to include them in the numerical models used in design, even if in this case the impact of neglecting PTW on predicted loads was minor.

7. Conclusions

Junctions in SCL tunnels are recognized as a challenging to design.

The lack of field data from junctions has added to the sense of uncertainty. This was the motivation for installing a detailed monitoring system at two junctions at Crossrail's Liverpool St Station. The original distributed fibre optic sensor (DFOS) system installation and monitoring proved the viability of the technology in the tough environment of sprayed concrete linings. This was the first time ever that a DFOS system was installed in an SCL tunnel. The data obtained from the monitoring has opened the path to a deeper understanding of the strains in these complex SCL junctions. The research presented in this paper is a first step along this path.

The numerical modelling has demonstrated that current design approaches can predict the general shape and magnitude of the strains with a reasonable agreement with the DFOS measurements. From this one can infer that the prediction of lining forces by this model is reasonable. However, this monitoring has also shown that the actual strains tend to be more localised that the numerical modelling predicts. Furthermore there are some significant areas of discrepancy – notably above and below the openings – and further work is required to understand the reasons for this.

The examination of excavation sequence suggests that simpler sequences could be used which would significantly simplify construction as well as reducing cost and embodied carbon. For example, the pilot tunnel in this case could have been omitted. The small changes in ground movements and lining loads associated with these simpler sequences do not suggest that there would be any detrimental impact on either the control of settlements and the protection of adjacent structures or the structural integrity of the parent tunnel.

Latter stages of this research have focussed on the constitutive modelling of the concrete lining and the simulation of the excavation process. The results from that work will be presented in future papers. Looking ahead, future site work could include the installation of fibre optic cables at different depths in the cross-section of a lining at a junction to record the bending strains. This is vital in order to understand the bending moments which generally govern the design of the reinforcement of tunnel junctions. In cases like these tunnels in London clay, which undergo a consolidation process in the long term, ideally these measurements would be conducted over a number of years to determine how the strains change in the lining over time. Monitoring of the SCL of the receiving parent tunnel would also be useful in corroborating the indications derived from this modelling that the strains in the receiving tunnels are less than those in the parent tunnel from which the cross-passage breaks out.

CRediT authorship contribution statement

Alun Thomas: Conceptualization, Formal analysis, Methodology, Writing – original draft, Writing – review & editing. **Mohammed Elshafie:** Funding acquisition, Writing – reviewing & editing. **Nicky de Battista:** Writing – reviewing & editing. **Giulia Viggiani:** Funding acquisition, Writing – reviewing & editing.

Declaration of Competing Interest

The authors declare that they have no known competing financial interests or personal relationships that could have appeared to influence the work reported in this paper.

Data availability

Data will be made available on request.

Acknowledgements

This research was performed at the Centre for Smart Infrastructure and Construction (CSIC) at Cambridge University with funding from the UK Engineering and Physical Sciences Research Council (EPSRC) and Innovate UK, under EPSRC grant nos. EP/N021614/1 and EP/I019308/1. Crossrail Ltd. has supported this project at all stages from the installation of the instrumentation through to this latest phase of research. The authors would like to acknowledge the support of the lead designer, Mott MacDonald, and main contractor, BBMV, a joint venture between Balfour Beatty, Beton- und Monierbau (BeMo), Morgan Sindall and Vinci Construction.

References

Arasteh, M., 2018 Crossrail Project, Farringdon Station, Design and Construction of the Primary Lining Tunnels SCL Junctions, British Tunnelling Society March 2018 Evening Presentation.

Chortis, F., Kavvadas, M., 2020. Three-Dimensional Numerical Analyses of Perpendicular Tunnel Intersections. Geotech Geol Eng. https://doi.org/10.1007/s10706-020-01587-w.

Clayton, C.R.I., Hope, V.S., Heyman, G., van der Berg, J.P., & Bica, A.V.D., 2000. "Instrumentation for monitoring sprayed concrete lined soft ground tunnels", Proc Instn Civ Eng Geotech Engng, Vol. 143, July, pp 119 – 130.

Clayton, C.R.I., van der Berg, J.P., Heyman, G., Bica, A.V.D., Hope, V.S., 2002. The performance of pressure cells for sprayed concrete tunnel linings. Geotechnique 52 (2), 107–115.

de Battista, N., Elshafie, M. Z. E. B., Soga, K., Williamson, M. G., Hazelden, G. & Hsu, Y. S. 2015. Strain monitoring using embedded distributed fibre optic sensors in a sprayed concrete tunnel lining during the excavation of cross-passages, 7th International Conference on Structural Health Monitoring and Intelligent Infrastructure (SHMII7), Torino, Italy.

Diez, R., 2018. Crossrail SCL Design, Tunnels & Tunnelling International, March 2018, pp 22 – 24.

Gakis, A., Flynn, S. Nasekhian, A. & Spyridis, P. 2016. The role of inverse analysis in tunnel design, https://learninglegacy.crossrail.co.uk/documents/role-inverse-analysis-tunnel-design/.

Goit, C.S., Kovács, A. & Thomas, A.H. 2011. Advanced numerical modelling in tunnel design – the example of a major project in the UK, 2nd International FLAC/DEM Symposium, 14-16 February 2011, Melbourne, Australia, pp 117 – 126.

Grose, W.J. & Eddie, C.M. 1996. Geotechnical aspects of the construction of the Heathrow Transfer Baggage System tunnel, Geotechnical Aspects of Underground Construction in Soft Ground, (ed.s Mair & Taylor), Taylor & Francis, London, pp 269 – 276.

Hafez, N.M., 1995. Post-failure modelling of three-dimensional shotcrete lining for tunnelling. University of Innsbruck. PhD thesis.

Hill, N. & Staerk, A., 2016 Long-term settlement following SCL-tunnel excavation. https://learninglegacy.crossrail.co.uk/documents/long-term-settlement-following-scl-tunnel-excavation/.

HSE, 1996. Safety of New Austrian Tunnelling Method (NATM) Tunnels. Health & Safety Executive, HMSO, Norwich, UK. ISBN 9780717610686.

ICE, 1996. Sprayed Concrete Linings (NATM) for tunnels in soft ground. Institution of Civil Engineers design and practice guides. Thomas Telford, London, ISBN 0727725122.

Jones, B.D., Clayton, C.R.I., 2020. 2020 Interpretation of tangential and radial pressure cells in and on sprayed concrete tunnel linings. Underground Space. https://doi.org/10.1016/j.undsp.2020.12.001.

Jones, B. D. 2007. Stresses in sprayed concrete tunnel junctions, Civil Engineering. University of Southampton. Available at: http://ethos.bl.uk/OrderDetails.do?uin=uk.bl.ethos.438713.

Kechavarzi, C. ,Soga, K., De Battista, N., Pelecanos, L., Elshafie, M. & Mair, R. 2016 Distributed Fibre Optic Strain Sensing for Monitoring Civil Infrastructure – a practical guide, Thomas Telford, ISBN: 9780727760555.

Kropik, C., 1994. Three-Dimensional Elasto-Viscoplastic Finite Element Analysis of Deformations and Stresses Resulting from the Excavation of Shallow Tunnels, PhD Thesis, TU Wien.

Li, Y., Jin, X., Lv, Z., Dong, J., Guo, J., 2016. Deformation and mechanical characteristics of tunnel lining in tunnel intersection between subway station tunnel and construction tunnel. Tunnell. Undergr. Space Technol. 56 (2016), 22–33.

Staerk, A., Jimenez-Rangel, L., & Wade, C., 2016 Analyses of convergence and utilisation of SCL-tunnels during excavation. https://learninglegacy.crossrail.co.uk/documents/analyses-convergence-utilisation-scl-tunnels-excavation/.

Thomas, A.H., 2003. Numerical modelling of sprayed concrete lined (SCL) tunnels. University of Southampton. PhD Thesis.

Thomas, A.H., 2021. The design of the Crossrail tunnels in the UK. Geomech. Tunnell. 14 (4), 340–346. https://doi.org/10.1002/geot.202100014.

Thomas, A.H., Powell, D.B. & Savill, M., 1998 Controlling deformations during the construction of natm tunnels in urban areas, Underground Construction in Modern Infrastructure, Franzen, Bergdahl and Nordmark (eds), pp 207 – 212.

Thomas, A.H., 2019 "Sprayed concrete lined tunnels," CRC Press London, ISBN: 9780429264566.

Van der Berg, J.P., 1999. Measurement and prediction of ground movements around three NATM tunnels. University of Surrey. PhD Thesis.